Effects of processing conditions on powder particle size and morphology in centrifugal atomisation of tin

J. W. Xie, Y. Y. Zhao and J. J. Dunkley

This paper investigates the effects of atomiser design and processing parameters on the morphology and size distribution of centrifugally atomised tin powder. Premature solidification of the melt on the atomiser and poor wetting of the atomiser by the melt were found to be the main causes of unsuccessful atomisation. The particle size distributions of the powders follow a lognormal distribution. The median particle size increased with decreasing atomiser rotation speed and with increasing melt flowrate. Cups with a high included angle made significantly finer powders than flat discs under the same operating conditions.

PM/1053

Dr Xie (jxie@liv.ac.uk) and Dr Zhao are in the Department of Engineering, The University of Liverpool, Liverpool L69 3BX, UK. Mr Dunkley is with Atomising Systems Ltd., Unit 8, M1 Distribution Centre, Meadowhall, Sheffield S9 1EW, UK. Manuscript received 10 March 2003; accepted 27 November 2003.

Keywords: Centrifugal atomisation, Atomisers, Powder, Particle size distribution

INTRODUCTION

Considerable technical and commercial developments of the centrifugal atomisation technique have been made in the past 30 years for producing metal powders, due to its advantages over conventional two fluid atomisation processes, such as spherical particles, narrow particle size distribution and low production cost. It has been successfully used for processing a wide range of metals, including Sn, Pb, Al, Mg, Ti, Ni, Co and their alloys. Yule and Dunkley have reviewed the development and applications of the centrifugal atomising processes and the relevant techniques used to characterise the atomised powders.[1] However, there is still a lack of a full scientific understanding of the process because of the complexity of the flow and disintegration of the melt on the atomiser.

Centrifugal atomisation is reported to occur in three typical modes: direct droplet formation, ligament disintegration and film disintegration. Hinz and Milborn proposed an empirical equation to describe the transition from one mode to another, but the mechanisms of the transitions are still not clear.[2] In the direct droplet formation regime, the droplet sizes as a function of atomising conditions can be predicted theoretically.[3,4] When ligament and film disintegration become the predominant mechanisms, however, the droplet size distribution can only be predicted by empirical expressions for some specific liquids in a certain range of atomising conditions.[5] As the atomising mode depends critically upon the liquid flow conditions on the atomiser, it is critical to understand the behaviour of the liquid flow on the disc in order to obtain powders with the desired properties. The flow behaviour of the melt in centrifugal atomisation is usually complicated. Mathematical modelling can be used to calculate the thickness and velocity profiles of the liquid metal film and thus to predict or explain the experimental results, such as particle shape and size distribution.[6–8] However, these models need to be experimentally validated before they can be used with confidence.

Sufficient wetting of the atomiser by the molten metal is essential for rapid acceleration and consequently effective disintegration of the melt. In the centrifugal atomisation of Mg alloys, poor wetting of the atomising disc or cup by the Mg alloys was found to be a major cause of failure of atomisation.[9,10] Thin coatings of other metals, such as Ca, Zn, Cu and Ni, could promote wetting of a steel atomiser by nearly all Mg alloys,[9] but excellent wetting was obtained by using atomisers with a coating of composition similar to that of the atomised alloy.[10,11] Cup shaped atomisers[12] were also used to improve the wetting between the melt and the atomiser and therefore to achieve a maximum liquid velocity. Although many different designs of atomiser rotors have been tried, no systematic investigations into the effect of shape on performance have been published.

This paper reports the effects of the atomiser design and the processing parameters on the morphology and size distribution of tin particles made in centrifugal atomisation, and studies the transitions in the modes of melt disintegration by high speed imaging.

EXPERIMENTAL PROCEDURE

The experiments were carried out in a simple air atmosphere laboratory rig with the atomiser driven by an electric motor with a variable speed of up to 18 000 rev min^{-1}. Commercially pure Sn was used as the model metal because of its low melting point and relatively good resistance to oxidation in air. In the experiments, Sn was first melted in a furnace at a temperature of 550°C to ensure a high superheat. The melt was then poured into a tundish with an exchangeable bottom nozzle. The melt flowed through the nozzle onto the atomiser disc under gravity. The mass flowrate of the melt was controlled by the orifice diameter of the nozzle. Three nozzles, with orifice diameters of $d = 2$, 3 and 4 mm, corresponding to melt flowrates of approximately 65, 150 and 220 kg h^{-1}, were used. The melt was accelerated by the rapidly rotating disc and broken up into a horizontal spray of droplets. A part of the spray was allowed to fly into a powder collection chamber, where the droplets solidified, mostly during flight, to form solid particles. A sample of the powder was finally collected for sieve analysis. The particle shape of the powder was characterised by a scanning electron microscope.

 DOI 10.1179/003258904225015482

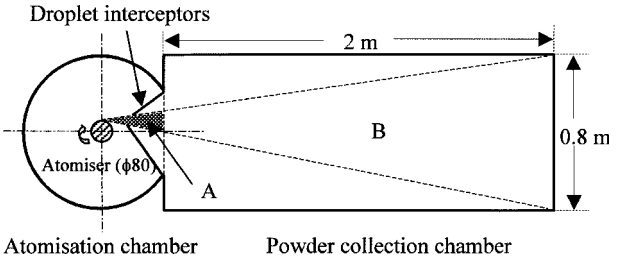

1 Schematic of centrifugal atomisation apparatus and sampling areas

Precautions have been taken in collecting the powder samples in the centrifugal atomisation experiments to avoid problems caused by the small dimensions of the rig. Figure 1 shows a schematic diagram of the atomisation and powder collection chambers used in the experiments. Only those particles settling in the area A in the atomisation chamber and the collection chamber B were collected for analysis. It was observed that the extremely fine droplets in the spray solidified rapidly and fell to the bottom of the atomisation chamber because they were subject to relatively large drag forces in flight. The flight of the coarser droplets was less affected by the air and the trajectories were nearly horizontal for a considerable flight distance. In the experiments, only about 5% of the atomised droplets entered the powder collection chamber through the gate in the wall of the atomisation chamber. A large proportion of the atomised droplets was intercepted by the circular wall of the atomisation chamber and froze to form a deposit. When the droplets impinged on the wall, secondary atomisation often took place. It was unavoidable that the powder sample in the atomisation chamber contained the splattered particles as a result of the secondary atomisation. In order to minimise the effect of the secondary atomisation and to exclude the splattered particles from the powder sample collected in both areas A and B, two interceptors were placed at the chamber gate, as shown in Fig. 1. The positions of the interceptors could be adjusted so that the droplets that entered the collection chamber had maximum flight distances before they impinged on the wall of the collection chamber. Although most droplets fully solidified before the impingement, some extremely large droplets were still partly liquid. These mushy droplets would break up further at the impingement and could distort the particle size distribution of the collected sample. It should also be pointed out that the turbulent airflow induced by the rapidly spinning atomiser, especially near the constrained gate region, had some influence on the eventual locations of the finest particles. These could drift with the airflow and settle at any location in the chambers. Despite the errors caused by the factors mentioned above, the effect was not significant. The samples collected in areas A and B should be close to representative of the powders produced in a single full size chamber under the same atomisation conditions.

A range of atomising disc designs was tried in the early stage. In the subsequent experiments, two types of atomisers were used: a flat disc and cups with wall slopes θ of 45°, 67·5° and 90°, as shown in Fig. 2. Both the disc and the cups have a diameter of 80 mm. They were all pretinned in order to maximise the wetting with the melt during atomisation.

RESULTS AND DISCUSSION

Atomiser design

An initial series of trial runs was carried out using a variety of atomising discs made from either mild steel or aluminium with different surface treatments. These trial runs were unsuccessful mainly due to either premature solidification of the melt or poor wetting of the atomiser by the molten metal.

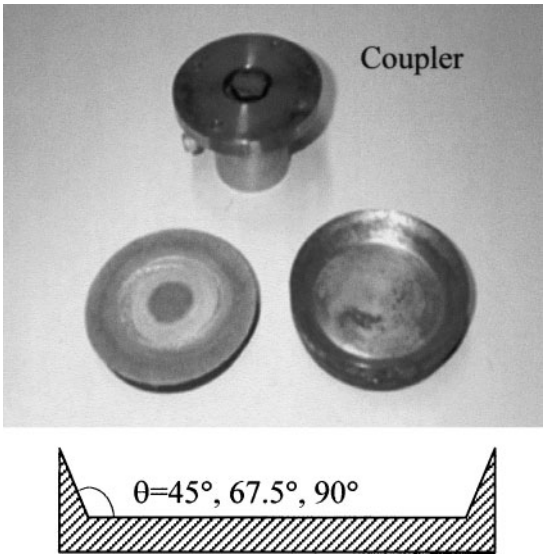

2 Atomiser coupler and typical discs used in present study

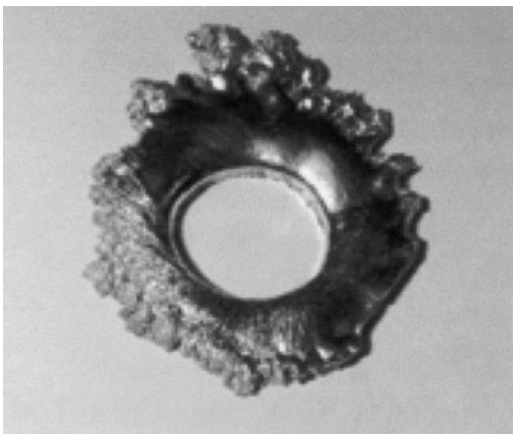

3 Typical skull formed on atomising disc

When the melt was poured onto a cold atomising disc rotating at a high speed, it spread rapidly into a thin film under the strong centrifugal force. A large fraction of the film solidified instantly as a result of heat conduction to the motor shaft and convective cooling by the surrounding air. This solidified thin film did not adhere to the surface of an untreated atomising disc and was broken up and thrown off as small flakes, leaving the atomising disc free from any residual metal.[13] Mechanically roughening the surface of the atomising disc resulted in temporary adherence of the solidified layer to the disc. As a consequence, a doughnut shaped solid skull, as shown in Fig. 3, was quickly built up on the atomising disc during atomisation. After reaching a certain size, the skull was often detached and thrown from the atomising disc as a result of centrifugal forces. The detachment of the skull in practical operations could damage the facility as well as radically affecting the geometry and atomisation behaviour. It is therefore desirable for the skull to be prevented in most cases. Coating the surface of the atomising disc with a 2 mm thick boron nitride layer showed no significant alleviation of the premature solidification of the melt. A skull still formed on the atomising disc, although it was not detached during the experiment because of the mechanical keying between the skull and the rough coating.

However, the surface of the atomising disc was not completely covered by the skull, indicating that, as expected, the melt did not wet the boron nitride coating. Increasing the amount of melt superheat was also found to be ineffective in eliminating premature solidification.

The skull formation problem was solved by the combination of two measures. A motor atomiser coupler, as shown in Fig. 2, was used to minimise the heat conduction to the motor shaft. At the same time, a hot air gun was installed to preheat the atomiser disc before atomisation and to maintain an elevated temperature during the operation. Although a solid layer still formed when the melt first impinged on the atomiser, it was melted by the hot metal flow within 10–15 s. Thereafter, the atomiser remained free of a solid skull throughout the experiment. Complete wetting of the disc by the melt was achieved by pretinning the atomiser before the experiment. These measures were found to be sufficient in maintaining an effective and satisfactory atomisation condition and were used for all the subsequent experiments.

Modes of atomisation

Depending upon the melt flowrate and the atomiser rotation speed, there are reported to be three modes of liquid disintegration in centrifugal atomisation, i.e. direct drop formation (DDF), ligament disintegration (LD) and film disintegration (FD). To predict the critical flowrates of the melt corresponding to the transitions between the three modes, Q_t an empirical relation (1) proposed by Champagne and Angers[14,15] was used in this work

$$Q_t = \frac{K\gamma^{0\cdot88}D^{0\cdot68}}{\mu^{0\cdot17}\omega^{0\cdot6}\rho^{0\cdot72}} \quad . \quad . \quad . \quad . \quad . \quad . \quad . \quad . \quad . \quad . \quad (1)$$

where D is the diameter of the atomiser in m, ω is the atomiser rotation speed in rad s^{-1}, γ is the surface tension of the melt in N m^{-1}, ρ is the density of the melt in kg m^{-3}, μ is the dynamic viscosity of the melt in Pa s^{-1} and K is a constant, which is 0·07 for the transition from DDF to LD and 1·33 for the transition from LD to FD. The calculated critical mass flowrates for the DDF–LD and LD–FD transitions in the present work, Q_{DDF-LD} and Q_{LD-FD}, respectively, at a few selected atomiser rotation speeds, are given in Table 1. In the experiments, three mass flowrates, 65, 150 and 220 kg h^{-1}, were used for each atomiser rotation speed. A comparison of the mass flowrates used in this work with the calculated transition mass flowrates indicates that the atomisation is likely to be in the ligament disintegration mode in most cases.

A SensiCam high speed imaging system consisting of a fast shutter speed CCD camera and a long focal distance microscope was used to observe the disintegration of the melt in centrifugal atomisation. Figure 4 shows two typical images of the melt flow on an early atomising disc with an untreated surface. It can be seen that the melt flow on the disc was very complex. The atomisation mode at the edge of the disc is not clearly of one type. There also seemed to be significant melt slippage on the untreated disc.

Particle morphology

Figure 5 shows the morphology of the particles for a typical powder sample. The particles appeared in various irregular shapes, from spherical, granular, short rod to needlelike. The finest particles, <10 μm, were usually almost spherical. The coarser particles were mainly in the form of short rods. Their aspect ratio ranged up to 12, but was largely between 2 and 6. No conclusive pattern of influence of operating parameters on shape was evident.

The fact that the particles were irregular rather than spherical in shape was due to the limitations of the current apparatus. All the experiments were carried out in air. As a consequence, there was rapid oxidation of the melt leading to the ligaments rapidly acquiring hard oxide shells preventing them from spherodising and possibly also inhibiting further disintegration. Particle morphology could certainly be improved by using an inert atmosphere.

Excessive cooling of the melt on the disc surface might also have some adverse effects on the atomisation, because there might not be sufficient time for the ligaments to disintegrate prior to freezing. Other researchers have found irregular particles in Al and Mg alloy powders produced by centrifugal atomisation.[16] Angers *et al.*[11,12] reported that these irregular particles formed from a small fraction of the

Table 1 Critical mass flowrates Q_{DDF-LD} and Q_{LD-FD} calculated by equation (1)

Rotation speed, rev min^{-1}	3000	6000	9000	12000	15000
Q_{DDF-LD}, kg h^{-1}	33	22	17	14	13
Q_{LD-FD}, kg h^{-1}	624	412	323	272	238

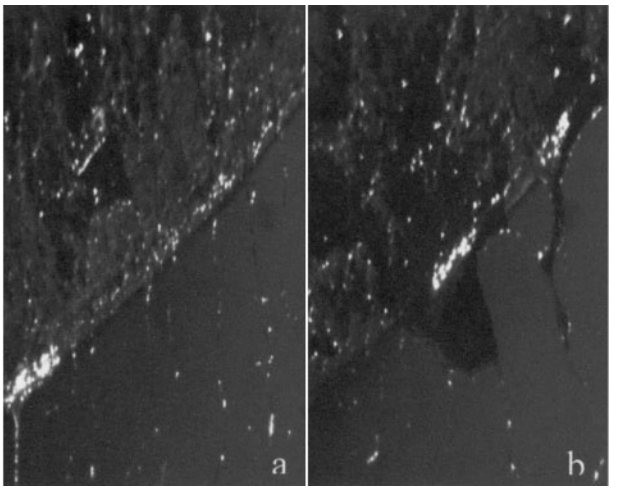

a 60 kg h^{-1} at 3320 rev min^{-1}; *b* 150 kg h^{-1} at 790 rev min^{-1}

4 High speed video images of melt on atomiser

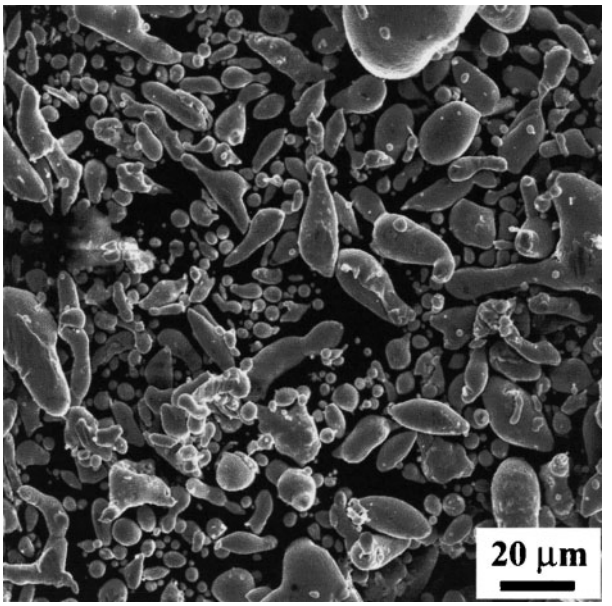

5 Morphology of particles of typical powder sample produced using 45° cup atomiser at rotation speed of 12 000 rev min^{-1}

melt, which solidified over the outer surface of the atomiser and broke up into small and irregular particles during atomisation.

Particle size distribution

Particle size distribution is the most important property of a powder. In centrifugal atomisation it is reported to depend on parameters such as the physical properties of the melt, its mass flowrate, the geometry and surface condition of the disc, and its speed. In this work, the effects of the melt flowrate, disc speed and disc/cup wall slope were investigated systematically. In any one group of experiments, only one parameter was varied with the others being fixed. Each of the as produced powder samples was sieved into a series of size groups and weighed. However, due to a large concentration of flakes and splats, believed to arise during startup or due to wall collisions, all particles larger than 425 μm were discounted. There are also problems with the fact that the equivalent spherical diameter of sieved particles varies greatly if they are spherical or heavily deformed, especially splatted or flaked. Thus, the resulting size distributions are somewhat distorted from the ideal.

Figure 6 shows plots of the cumulative weight percentage of the particles versus particle size for the powder samples produced using a flat atomising disc for different melt mass flowrates at 6000–15 000 rev min^{-1}. All the samples showed a reasonably linear plot on this lognormal scale, although deviations are evident. The distributions obtained in all experiments were thus plotted in this way and the mass median particle size plotted against disc speed and melt flow is shown in Fig. 7. It can readily be seen that the effect of melt flowrate on size is most pronounced at low rotation speeds, while at the highest speeds it becomes quite slight.

In addition to the experimental data, Fig. 8 shows trend lines for a simple reciprocal relationship between median particle size and disc speed, which is reported by other authors. The trend lines are the best fit curves to the data by using $d_m = k/\text{speed}$. The values of k corresponding to melt flowrates of 65, 150 and 221 kg h^{-1} are 0·927, 1·2 and 1·53x10^6 (μm/rev min^{-1}), respectively. It can be seen that k is nearly proportional to melt flowrate. The data for melt flowrate of 150 kg h^{-1} follows the reciprocal relationship very well, while the data for 65 kg $h^{-1}$and for 221 kg h^{-1} agree with such a relationship less well.

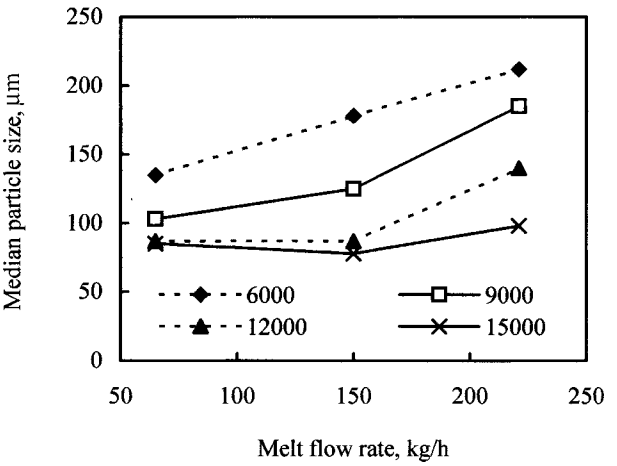

7 Effect of melt flowrate on median particle size at difference disc speeds

It is also found, when examining the particle size distribution curves, that the standard deviation of the distribution is far larger than reported elsewhere for centrifugal atomisation, where values of 1·3–1·5 are normal. The present data show very variable values in the range 1·7–3·0. This could be for several reasons: the inhibition of breakup by the oxide films formed, the short duration of experiments, leading to large startup and end effects, and the limitations of the powder collection system.

Figure 9 shows the powder size as affected by the cup geometry at atomiser rotation speeds of 6000 and 12 000 rev min^{-1} for a nozzle diameter of 4 mm. There is a distinct trend towards finer powders as the angle of the cup wall increases to 67·5 degrees to the horizontal, but it

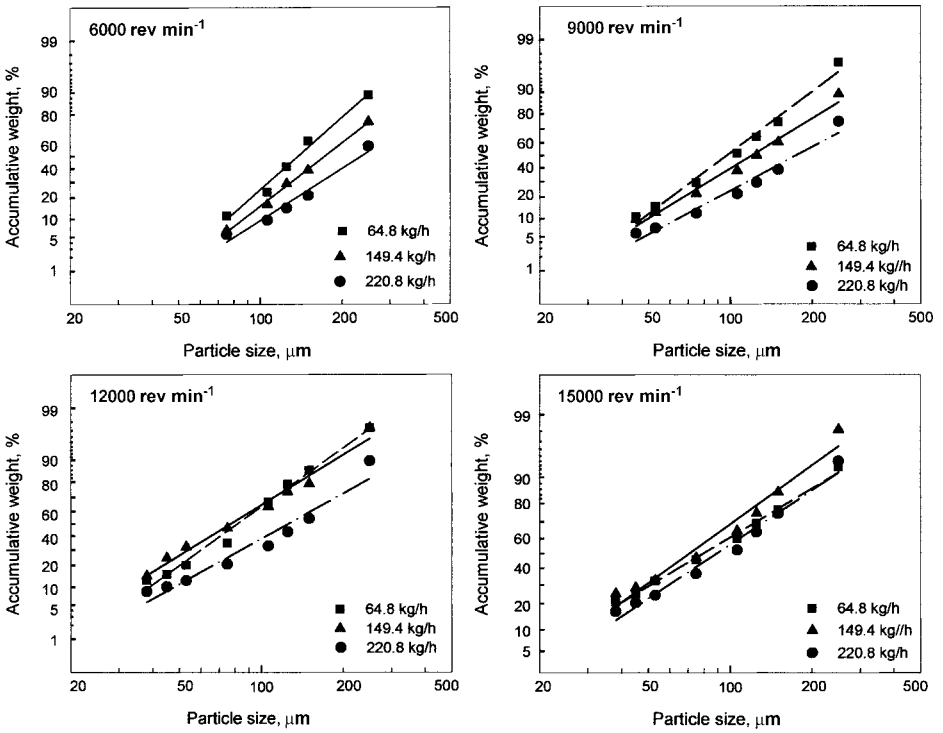

6 Particle size distributions of powder samples produced at different mass flowrates of melt

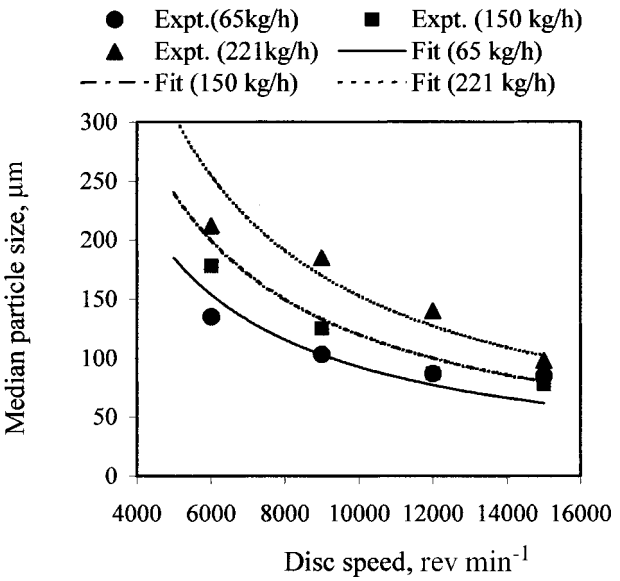

8 Median particle size versus disc speed

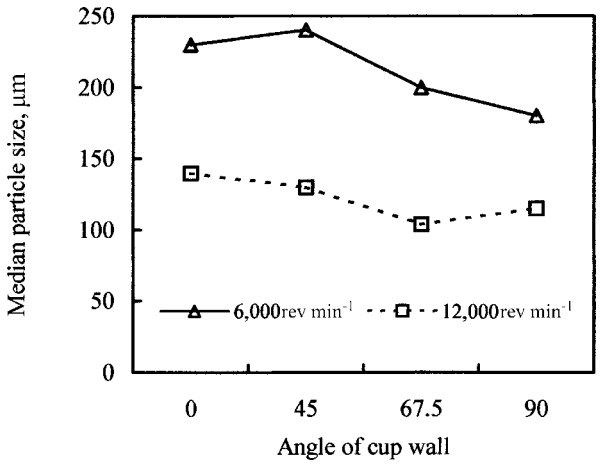

9 Median particle size at 220 kg h^{-1} and two cup speeds as a function of cup angle

is not clear if 90 degrees leads to finer particles for 12 000 rev min^{-1}. The use of a cup, as opposed to a flat disc, in the conditions used here, appears to reduce particle size by as much as 25% in the case of the higher speed, and by 20% for the lower speed.

Effects of melt flow pattern

The data presented above can be understood intuitively by considering the effects of the flow of metal, the speed of the disc and how they interact. Clearly, if the radial velocity of the melt film is constant, then the higher the melt flowrate, the thicker the film on the disc. This makes the acceleration of the film more difficult as the thicker film shears under lower stress and the melt is more likely to slip on it and fail to reach the disc velocity at its periphery. As the disc speed increases, the film thickness will drop at constant flowrate. This will reduce the effect of flowrate on slip. In this way, one can understand why the curves for different flowrates converge at higher speeds in Fig. 8.

The same line of argument can be used to explain the beneficial effect of the higher angle cup geometry. The liquid film will be much more effectively flattened down to the surface by the centrifugal force at the cup wall, and this should make it accelerate and perhaps become more uniform in thickness. The fact that this effect exists points to the film thickness and wetting behaviour being far from ideal. Theoretical formulae for film thickness indicate that it should be of the order of 3–8 μm under the reported conditions. It is very difficult to imagine such a thin film suffering from any slip, as the shear rate in it would be very high. It is thus likely that flow is markedly non-uniform and not in the form of a uniform thin film. However, interference from oxidation could be very significant in this work, so only tentative conclusions are possible.

CONCLUSIONS

1. Powders produced in air had irregular particle shapes. This was due to the oxidation of the melt during atomisation.
2. Particle sizes of the powders produced by centrifugal atomisation followed a roughly lognormal distribution.
3. The mass median particle size of the powder was mainly dependent upon the atomiser rotation speed and the mass flowrate of the melt. Particle size increased with decreasing atomiser rotation speed and with increasing melt flowrate.
4. The use of cups with steep walls was shown to reduce particle sizes by as much as 25% compared with a flat disc.

ACKNOWLEDGEMENTS

This work was supported by the EPSRC and Atomising Systems Ltd. JWX and YYZ would like to thank Dr D. Sun and Mr D. Whitehurst for their assistance in carrying out the experiments.

REFERENCES

1. A. J. YULE and J. J. DUNKLEY: 'Atomisation of metals for powder production and spray deposition'; 1994, Oxford, Clarendon Press.
2. J. O. HINZ and M. MILBORN: *J. Appl. Mech.*, 1950, **17**, (2), 145–153.
3. Y. TANASAWA, Y. MIYASAKA and U. UMEHARA: Proc. 1st Int. Conf. on 'Liquid atomisation and spray systems', Tokyo, Japan, 1978, Fuel Society of Japan, 165–172.
4. A. R. E. SINGER and S. E. KISAKUREK: *Met. Technol.*, 1976, **3**, 565–570.
5. R. P. FRASER, E. P. EISENKLAM and N. DOMBROWSKI: *Brit. Chem. Eng.*, 1957, 496–501.
6. Y. Y. ZHAO, M. H. JACOBS and A. L. DOWSON: *Metall. Mater. Trans. B*, 1998, **29B**, 1357–1369.
7. Y. Y. ZHAO, A. L. DOWSON, R. M. WARD and M. H. JACOBS: 'PM'98: world congress on powder metallurgy', Vol. 1, 8–13; 1998, Shrewsbury, EPMA.
8. H. P. LI and P. TSAKIOPOULOS: *Key Eng. Mater.*, 2001, **189/191**, 245–251
9. J. N. REDING: U.S. Patent 3, 520, 718, July 14, 1970.
10. R. S. BUSK: *Light Met.*, 1960, **23**, 197–201.
11. R. ANGERS, D. DUBE and R. TREMBLAY: *Int. J. Powder Metall.*, 1994, **30**, 429–433.
12. R. ANGERS, R. TREMBLAY, L. DESROSIERS and D. DUBE: *Can. Metall. Q.*, 1996, **35**, (3), 291–297.
13. F. FOLIO and A. LACOUR: *Powder Metall.*, 2000, **43**, (3), 245–252.
14. B. CHAMPAGNE and R. ANGERS: in 'Modern developments in powder metallurgy', (eds. H. H. Hausner *et al.*), Vol. 12, 83–104; 1981, Princeton, NJ, MPIF.
15. B. CHAMPAGNE and R. ANGERS: *Powder Metall. Int.*, 1984, **16**, 125–128.
16. C. LABRECQUE, R, ANGERS, R. TREMBLAY and D. DUBE: *Can. Metall. Q.*, 1997, **36**, (3), 169–175.